

# APPLICABILITY OF BITUMINOUS-BASED INHIBITOR AS CORROSION PREVENTION METHOD IN REINFORCED CONCRETE

Pinta Astuti

Universitas Muhammadiyah Yogyakarta, Department of Civil Engineering, Jalan Brawijaya, Tamantirto, Kasihan, Bantul, Daerah Istimewa Yogyakarta, Indonesia

\* pinta.astuti@ft.umy.ac.id

Corrosion is the most common cause of structural and material degradation in reinforced concrete (RC) constructions. A well-constructed structure protects the embedded steel bar from chloride ions both physically and chemically, which is particularly important for constructions exposed to seawater. Given the significant economic losses caused by corrosion, suitable measures to reduce corrosion in concrete are required. In this study, three-layer of bituminous-based inhibitor was applied to the surface of two steel bars embedded (steel coating) in mortar cement with 3 cm and 5 cm of concrete cover. Portland composite cement (PCC) and Portland pozzolan cement (PPC) was used as a binder material of mortar cement. The cubical mortar cement specimens were fabricated, and exposed to three conditions (e.g., wet condition, dry condition, and dry-wet cycle) until 60 days after 28 days of immersed water curing. The results demonstrated that corrosion prevention employing steel coating techniques by using bituminous-based inhibitor gives superior protection as seen by a higher positive corrosion potential value when compared to non-coating specimens, implying that the coating method may be used to prevent corrosion. This is because the coating process by using bituminous-based inhibitor may prevent ions from entering the reinforcing steel. In all exposure circumstances and with all preventive procedures, a concrete cover with a thickness of 5 cm has a lower corrosion risk, as shown by a higher corrosion potential value, than a concrete cover with a thickness of 3 cm. The larger the thickness of the concrete cover, the more the surrounding ecosystem is protected. The utilization of PPC as binder in concrete maintained the stable corrosion potential value when the coating method applied.

Keywords: bituminous-based inhibitor, corrosion prevention, half-cell potential, PCC, PPC

## 1 INTRODUCTION

Reinforced concrete (RC) is the most intensive utilized material for building structures in the world [1, 2]. However, there are many factors affecting the deterioration process, such as corrosion of steel bars so that the service life of structures is significantly decreased [3, 4]. In the immunity condition of the concrete, a passive oxide layer over the steel surface is produced, and the highly alkaline concrete pore solution protects the steel reinforcement from aggressive ions [1, 5]. The passive layer, on the other hand, may be damaged, and corrosion of steel reinforcement can begin owing to carbonation or the presence of a significant amount of chloride ions at the rebar level [1, 2, 6, 7]. The corrosion of steel reinforcement caused by chloride impacts the durability and service life of reinforced concrete buildings exposed to harsh conditions, resulting in significant repair and maintenance expenditures [1][8], [9]. A well-constructed RC structure protects the embedded steel bar from chloride ions both physically and chemically, which is particularly important for constructions exposed to a seawater environment [1]. Due to the significant economic losses caused as a result of corrosion, suitable measures to reduce corrosion in concrete are required [1, 10]. There are several prevention methods to control corrosion, such as the application of corrosion inhibitors, cathodic prevention, electrochemical re-alkalization, etc. In terms of applicability and cost-effectiveness, corrosion inhibitors have shown to be an efficient means of reducing corrosion rates [11].

The number of studies on new corrosion inhibitor materials has grown gradually [12, 13, 14, 15, 16, 17, 18]. Many chemical ingredients of commercially available corrosion inhibitors such as potassium fluorosilicate, amine carboxylate, nitrite, phosphate-based, etc. Overall, inhibitors based on potassium fluorosilicate and amine carboxylate demonstrated the greatest resistance to stray current [19]. The greater the concrete strength over 3.6 V electrical potential, the more effective the corrosion prevention [19]. In corrosion kinetics, there are five stages that describe the change in electrical resistance of a reinforced concrete sample: Corrosion initiation, corrosion filling phase, crack development, crack propagation, and collapse of structure [19]. When a fracture that corresponds to the margins is formed, the advantages of corrosion inhibitors are negligible [19]. Electrochemical measurements were used to determine the effectiveness of nitrite and phosphate-based inhibiting admixtures, specifically sodium nitrite ( $\text{NaNO}_2$ ) and di-Sodium hydrogen phosphate ( $\text{Na}_2\text{HPO}_4$ ), against corrosion of reinforcing steel in concrete exposed to a chloride environment with various chloride content levels [20]. Compared to ordinary Portland cement (OPC), the production of denser microstructure in concrete formed with Portland pozzolan cement (PPC) was more influential in reducing the amount of corrosion than the influence of inhibitory admixtures [20]. Organo-functional silanes, Amino-alcohol, and Surfactant & amine salts-based inhibitors were evaluated in the United Kingdom, with organo-functional silanes-based inhibitors demonstrating the highest inhibitor effectiveness and barrier qualities [11]. Novel inhibitor-loaded functional HNTs-modified coatings exhibit excellent anti-corrosion properties, and these findings provide new insights into the preparation of smart coatings, which are anticipated to find widespread application in the corrosion protection of steel and other metals in reinforced concrete environments [21].

In the previous study that was conducted to inject corrosion inhibitors into concrete at sufficiently high pressure, measure the penetration properties of corrosion inhibitors and the nitrite ion concentrations at various regions in the concrete by employing penetration theory, and clarify the corrosion inhibition mechanisms, water permeability of concrete, and concentration ratios of nitrate ions to chloride ions, the pressure and pressurizing time were determined to be optimal [22].

One of the potential materials to be corrosion inhibitors in concrete is bituminous-based paint. Bituminous material is extensively employed in the construction and building industry, which often requires superior waterproofing performance during application [23]. The influence of clay particles on the corrosion properties of the bituminous coating was studied by previous research [24], and the results showed that the addition of clay nanolayers improved the corrosion resistance of the coatings. But there is no previous research related to the utilization of bituminous paint as corrosion inhibitor material in new concrete construction or as a prevention method, so this research aims to clarify the effectiveness of bituminous based paint as steel coating in the view point of corrosion prevention in RC structures.

## 2 MATERIALS AND METHODS

### 2.1 Specimen design

The cubical mortar cement specimens with the dimension of 15 cm x 15 cm x 15 cm were fabricated. Two round steel bars of 12 mm in diameter were embedded in the depth of 3 cm and 5 cm from the top specimen's surface. Three types of binder variation were used in this experiment, e.g., 100% Portland composite cement (PCC), 100% Portland pozzolan cement (PPC), and 50% Portland composite cement (PCC) and 50% Portland pozzolan cement (PPC). No treatment and steel coating were applied to the steel bar surface to clarify the effectiveness of bituminous-based inhibitor as coating material. The summary of the specimen's variation is presented in Table 1.

Table 1. Variation of specimens

No.	Type of Binder	Prevention Method
1.	100% Portland composite cement (PCC)	No treatment
2.	100% Portland composite cement (PCC)	Steel coating
3.	100% Portland pozzolan cement (PPC)	No treatment
4.	100% Portland pozzolan cement (PPC)	Steel coating
5.	50% Portland composite cement (PCC) + 50% Portland pozzolan cement (PPC)	No treatment
6.	50% Portland composite cement (PCC) + 50% Portland pozzolan cement (PPC)	Steel coating

### 2.2 Properties of materials

The physical properties of fine aggregate used from Progo River, Kulon Progo, Daerah Istimewa Yogyakarta, Indonesia were tested by using the sieve analysis method as presented in Figure 1 and Table 2.

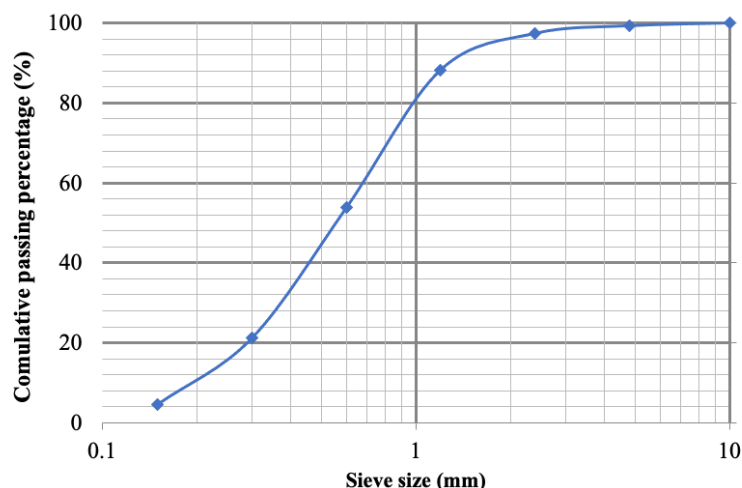


Fig. 1. Sieve analysis of fine aggregate

Table 2. Properties of fine aggregate

Characteristic	Observed Value	Code/Standard
Origin	Progo River sand	-
Aggregate type	Mild sand	-
Grade zone	II	SNI 1970:2016
Specific gravity	2.78 gram/cm <sup>3</sup>	SNI 1970:2016
Water absorption	2.56 %	SNI 1970:2016
Fineness modulus	2.039	

Table 3 Presents the properties of the binder material (Portland Composite Cement (PCC) and Portland Pozzolan Cement (PPC)) including the specific gravity (SNI 2531:2015), normal consistency (SNI 03-6826-2002), initial setting time (ASTM C403), and final setting (ASTM C403) based on the code or standard.

Table 3. Properties of binder

Characteristic	Observed Value		Code/Standard
	Portland Composite Cement (PCC)	Portland Pozzolan Cement (PPC)	
Type of binder	Portland Composite Cement (PCC)	Portland Pozzolan Cement (PPC)	
Specific gravity	3.35 gram/cm <sup>3</sup>	3.09 gram/cm <sup>3</sup>	SNI 2531:2015
Normal consistency	26.3%	36.2%	SNI 03-6826-2002
Initial setting time	86.2 minutes	32.8 minutes	ASTM C403
Final setting time	150 minutes	600 minutes	ASTM C403

The yield strength of two round steel bars with a diameter of 12 embedded in mortar cement is 436.13 MPa. The modulus elasticity is 222.382 MPa. The copper wire cable is connected to the end of each steel bar in order to measure the electrochemical test. The bituminous-based inhibitor used as steel bar surface coating before the specimen's fabricating is commercially available-anti corrosion paint. The density is 1.02 – 1.12 g/ml. The thickness per coat is 25 - 30  $\mu\text{m}$ . and theoretical coverage is 6 – 7 m<sup>2</sup> / l. The drying time is 30 - 40 minutes at 30 °C at touch dry and about 2 hours at 30°C at hard dry.

### 2.3 Mix design of mortar cement

The mix proportion of mortar cement is presented in Table 4.

Table 4. Mix proportion of mortar Portland pozzolan cement (PPC)

Material	Composition
PPC (kg/m <sup>3</sup> )	554.43
Fine Aggregate (kg/m <sup>3</sup> )	1663.3
Water (liter/m <sup>3</sup> )	221.8
Superplasticizer (liter/m <sup>3</sup> )	4.15

### 2.4 Curing period and exposure condition

One day after mixing and casting, the specimens were demolded, then it was cured and immersed in the tap water until 28 days. Three types of exposure conditions, including wet conditions by covering wet towels, dry laboratory air condition, and seawater dry-wet cycle (two days wet followed by five days dry), were started after the curing period to simulate the real condition of the concrete structure.

### 2.5 Fresh properties of mortar cement

In order to ensure the workability and homogeneity of fresh mortar cement, the flow table and density were tested [25, 26, 27, 28, 29, 30]. According to SNI 6882:2014, the allowed flow table value for the flow table test ranges from 105% to 115%. The flow table test is in accordance with ASTM C 1437-07 [31]. The average flow value is 112.67%, which fulfills the necessary flow value criterion. To ascertain the mass of each volume of concrete, density testing based on SNI 1973:2016 [32] was performed. Based on the test, the average density is 2080.68 kg/m<sup>3</sup> or 2.081 gr/cm<sup>3</sup>.

### 2.6 Hardened properties of mortar cement

The compressive strength test is conducted to the hardened mortar cement by using cylindrical specimens with 15 cm of diameter and 30 cm of height. The average result of PPC and PCC mortars are 22.59 MPa and 24.53 MPa, respectively.

### 2.7 Electrochemical test of specimens

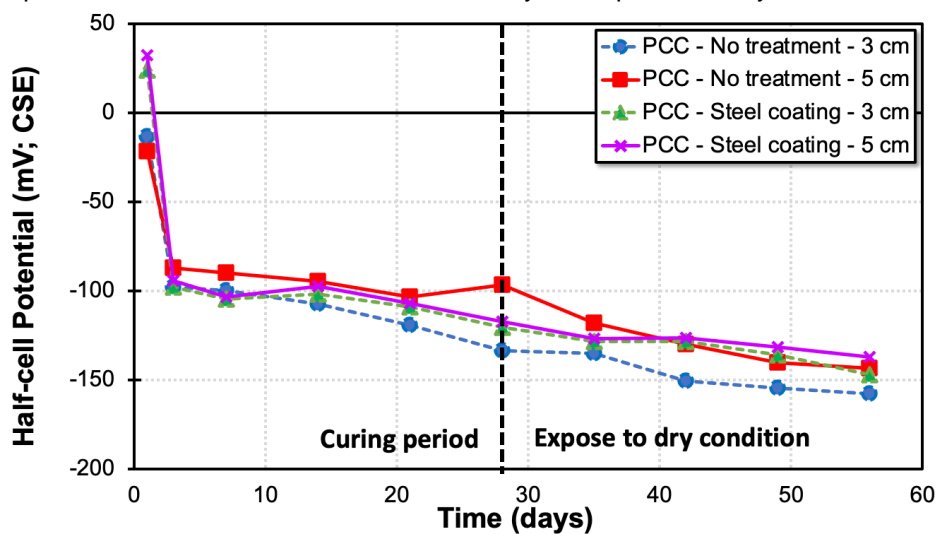
The American Standard ASTM C876 defines interpretation criteria for reinforced concrete structures exposed to the environment (e.g. bridge decks), which are summarized in Table 5. The values represent a particular circumstance, concrete type, and cover and are not generally applicable. Indeed, as theoretical considerations and practical experience on a large number of structures [33] have demonstrated, there are no absolute potential values to indicate the probability of corrosion in a structure, contrary to the interpretation provided in ASTM C876-91, which is based on a fixed potential value of -350 V CSE. Various potential ranges indicate corrosion of rebars in different constructions depending on moisture content, chloride concentration, temperature, carbonation of the concrete, and cover thickness. The gradient between corroding and passive zones is more relevant than the absolute magnitude of the potential in locating regions of corroding rebars.

In this experiment, silver-silver chloride electrode (SSE) was used as reference electrode during half-cell potential test. The detected potential value was converted to the calomel saturated electrode (CSE) as the standard value. Thirty minutes of pre-wetting by using tap water was sprayed to the specimen surface before measuring.

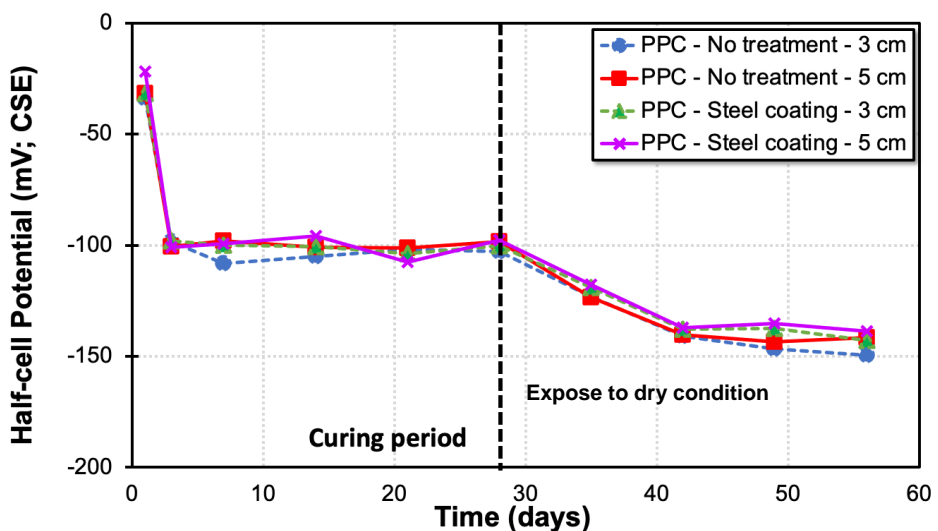
### 3 RESULTS AND DISCUSSIONS

#### 3.1 Half-cell potential of steel bar in dry exposure condition

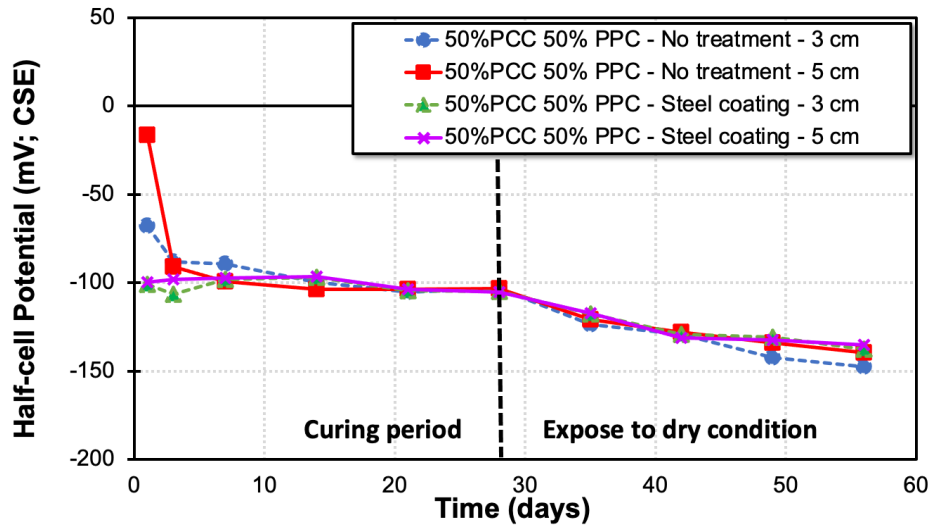
Half-cell potential of steel bar was measured on the concrete surface after 30 minutes of prewetting by using tap water. The measurement period of this research is 56 days including 28 days of curing and 28 days of exposure period. There are three type of exposure conditions e.g., dry condition, wet condition, and dry-wet cycle condition. The results of half-cell potential of steel bars during dry exposure condition were presented in Figure 2a-c. In these figures, 100% Portland composite cement (PPC), 100% Portland pozzolan cement (PCC), and combination 50% PPC and 50% PCC effects on the half-cell potential results of steel bars were depicted. Two comparison of corrosion prevention method by using bituminous based paint and none in the 3 cm and 5 cm concrete cover of steel bars were also described. In Figure 1-3a-c, potential corrosion values of steel bars in the curing period until 28 days shift to negative value. The specimens using PPC binder performed the worse condition than another cement. The PPC and the mixture of cement affected on the stable potential value in -100 mV vs CSE. It indicated that the chemical component of pozzolan in the PPC binder maintained the potential or steel bar during curing period. The Figure 2a depicted that the steel bar in PCC without coating embedded in 3cm of cover thickness present the worse condition indicated by the most negative potential value among others during exposure to dry condition. The specimens in PPC and mixture cements presents the potential value shifted to -145 mV vs CSE. There was no sign of corrosion indicated by half-cell potential based on ASTM C876 until 56 days of exposure in dry condition.



(a)



(b)

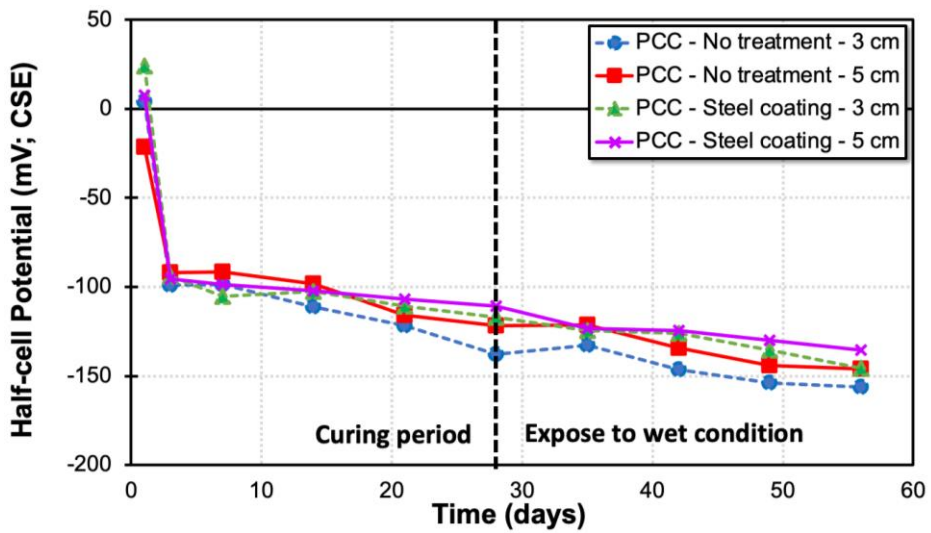


(c)

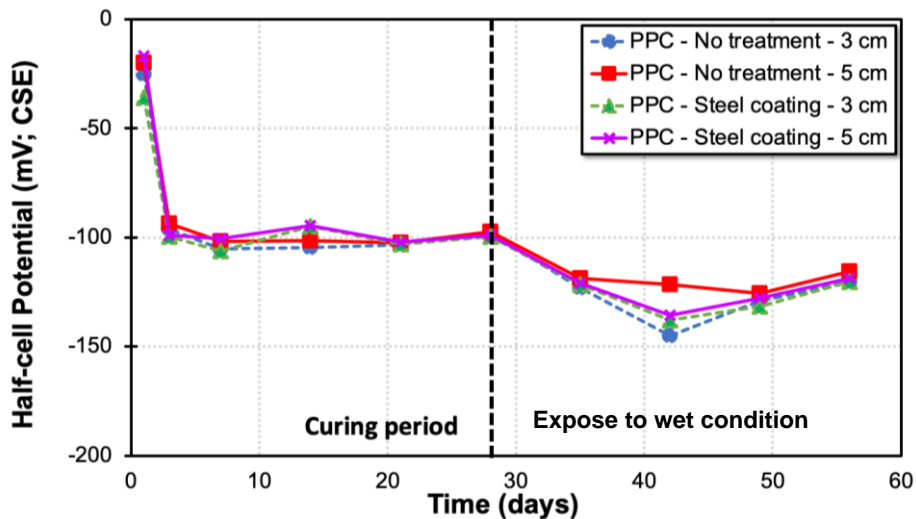
Fig. 2. Half-cell potential of steel bar in (a) PCC mortar, (b) PPC mortar, and (c) 50% PCC and 50% PPC mortar during dry exposure condition

### 3.2 Half-cell potential of steel bar in wet exposure condition

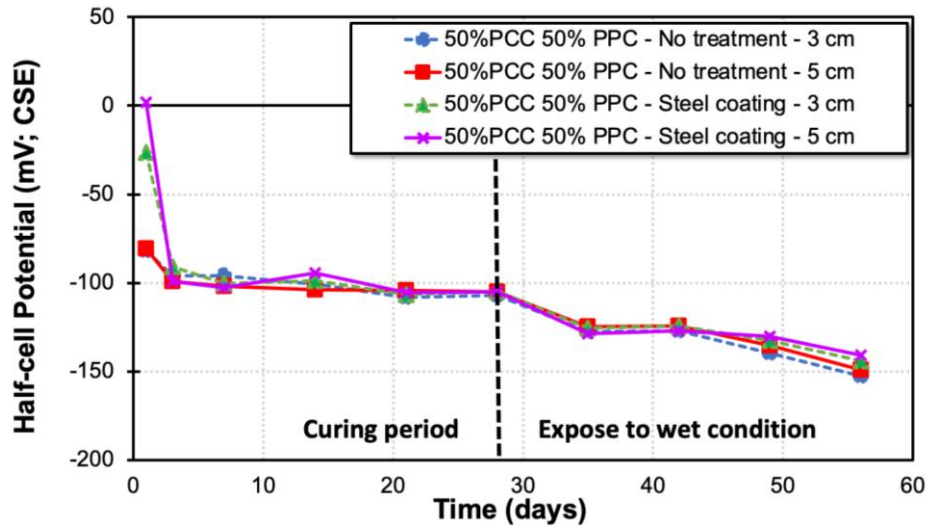
The results of half-cell potential of steel bars during wet exposure condition were presented in Figure 3.



(a)



(b)



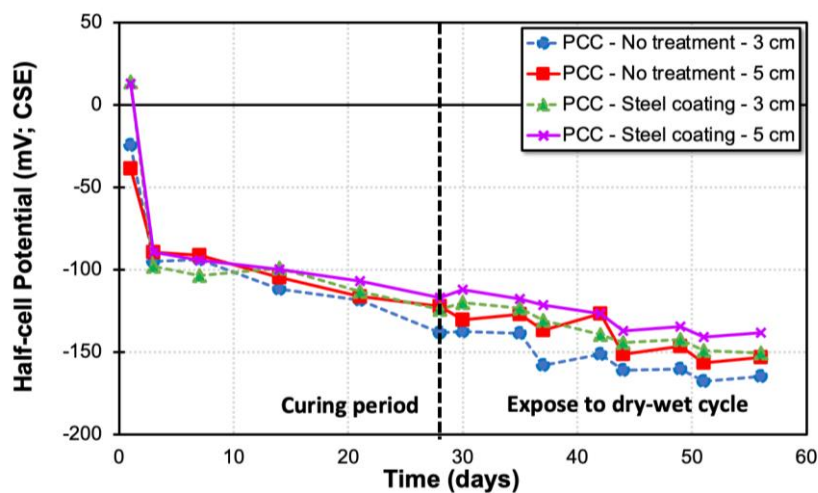
(c)

Fig. 3. Half-cell potential of steel bar in (a) PCC mortar, (b) PPC mortar, and (c) 50% PCC and 50% PPC mortar during wet exposure condition

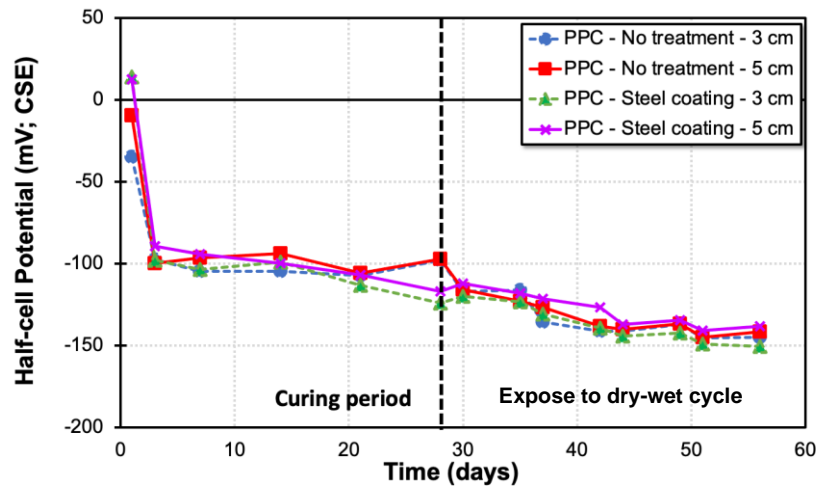
The potential of steel bar was continue shifted to negative value during wet exposure condition. The interesting phenomenon, only specimens using PPC as binder presented the potential recover and maintained the potential to -120 mV vs CSE as depicted in Figure 3b. The similar trend of coating as corrosion prevention and the concrete cover thickness were occurred. It was in good agreement with the condition in dry condition.

### 3.3 Half-cell potential of steel bar in dry-wet cycle exposure condition

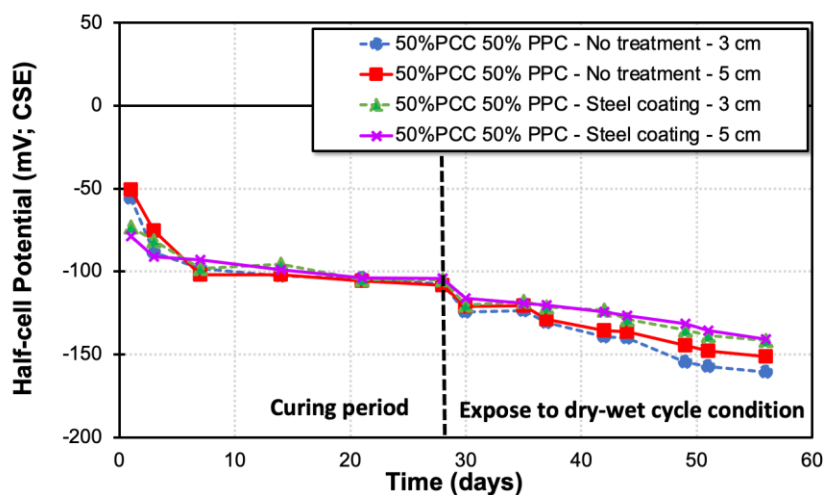
The results of half-cell potential of steel bars during dry-wet cycle exposure condition were presented in Figure 4. This exposure is the most severe condition to simulate the real tidal zone of reinforced concrete structure in sea water environment. The accumulation of chloride ions increased in this zone. The cement type used in the concrete mix was really affected to the corrosion performance of steel bar. Figure 4a and 4c presented the average potential value after 56 days of exposure was in below -150 mV vs CSE. The PPC binder could maintained the potential value stable in 150 mV vs CSE. All potential values in this experiment were categorized as 90% in no corrosion condition based on ASTM C876 due to the new steel bar was installed the only 56 days of exposure condition. This could be used to understand about the early performance of coating method as corrosion prevention.



(a)



(b)



(c)

Fig. 4. Half-cell potential of steel bar in (a) PCC mortar, (b) PPC mortar, and (c) 50% PCC and 50% PPC mortar during dry-wet cycle exposure condition

#### 4 CONCLUSION

Corrosion prevention using steel coating techniques provides superior protection, evidenced by a higher positive corrosion potential value compared to non-coated specimens. This suggests that the coating method, particularly using a bituminous-based inhibitor, is effective in preventing corrosion by blocking ions from reaching the reinforcing steel. A concrete cover of 5 cm thickness consistently shows a lower corrosion risk, indicated by a higher corrosion potential value, compared to a 3 cm cover, as a thicker cover better shields the surrounding environment. Specimens exposed to a dry-wet cycle exhibit the most negative corrosion potential values, while those under a constant dry condition show the highest corrosion potential. The corrosion potential value is more negative under wet conditions than dry ones. Portland Pozzolan Cement (PPC) binder maintains a stable corrosion potential value better than Portland Composite Cement (PCC) and PPC-PCC mixture up to 56 days of exposure.

#### 5 ACKNOWLEDGMENTS

The authors would like to acknowledge Research and Innovation Institute (LRI) Universitas Muhammadiyah Yogyakarta through 2022 Fundamental Research Scheme, Decree No. 56/R-LRI/XII/2022, who financially supports the research. The author also would like to thank Ms. Fanny, Ms. Fahma, Ms. Dyah, Ms. Ataya, Ms. Farah, Mr. Afdhal, Mr. Zakri, and Mr. Sumadi for their help.

#### 6 REFERENCE

- [1] Shehnazdeep, & Pradhan, B. (2022). A study on effectiveness of inorganic and organic corrosion inhibitors on rebar corrosion in concrete: A review. *Materials Today: Proceedings*. <https://doi.org/10.1016/j.matpr.2022.04.296>

- [2] Zhang, X., Zhang, Y., Liu, B., Liu, B., Wu, W., & Yang, C. (2021). Corrosion-induced spalling of concrete cover and its effects on shear strength of RC beams. *Engineering Failure Analysis*, 127, 105538. <https://doi.org/10.1016/j.engfailanal.2021.105538>
- [3] Dasar, A., Hamada, H., Sagawa, Y., & Yamamoto, D. (2017). Deterioration progress and performance reduction of 40-year-old reinforced concrete beams in natural corrosion environments. *Construction and Building Materials*, 149, 690–704. <https://doi.org/10.1016/j.conbuildmat.2017.05.162>
- [4] Meiyuan, H., Minghui, J., Wenlei, Z., Yubin, Y., Teng, C., & Hao, W. (2021). Composite salt corrosion deterioration characteristics and damage calculation models of concrete incorporated with corrosion inhibiting admixtures. *Journal of Building Engineering*, 44, 103221. <https://doi.org/10.1016/j.jobbe.2021.103221>
- [5] Rodrigues, R., Gaboreau, S., Gance, J., Ignatiadis, I., & Betelu, S. (2021). Reinforced concrete structures: A review of corrosion mechanisms and advances in electrical methods for corrosion monitoring. *Construction and Building Materials*, 269, 121240. <https://doi.org/10.1016/j.conbuildmat.2020.121240>
- [6] El Maaddawy, T., & Soudki, K. (2007). A model for prediction of time from corrosion initiation to corrosion cracking. *Cement and Concrete Composites*, 29(3), 168–175. <https://doi.org/10.1016/j.cemconcomp.2006.11.004>
- [7] Khan, M. U., Ahmad, S., & Al-Gahtani, H. J. (2017). Chloride-induced corrosion of steel in concrete: An overview on chloride diffusion and prediction of corrosion initiation time. *International Journal of Corrosion*, 2017, 1–9. <https://doi.org/10.1155/2017/5819202>
- [8] Astuti, P., Kamarulzaman, K., Rafdinal, R. S., Hamada, H., Sagawa, Y., & Yamamoto, D. (2020). Influence of rust removal process on the effectiveness of sacrificial anode cathodic protection in repair concrete. *IOP Conference Series: Materials Science and Engineering*, 849(1), 012088. <https://doi.org/10.1088/1757-899X/849/1/012088>
- [9] Astuti, P., Rafdinal, R. S., Hamada, H., Sagawa, Y., Yamamoto, D., & Kamarulzaman, K. (2019). Effectiveness of rusted and non-rusted reinforcing bar protected by sacrificial anode cathodic protection in repaired patch concrete. In *IOP Conference Series: Earth and Environmental Science*. <https://doi.org/10.1088/1755-1315/366/1/012013>
- [10] Loziquez, E., Barthélémy, J. F., Bouteiller, V., & Desbois, T. (2018). Contribution of sacrificial anode in reinforced concrete patch repair: Results of numerical simulations. *Construction and Building Materials*, 178, 405–417. <https://doi.org/10.1016/j.conbuildmat.2018.05.063>
- [11] Goyal, A., Ganjian, E., Pouya, H. S., & Tyrer, M. (2021). Inhibitor efficiency of migratory corrosion inhibitors to reduce corrosion in reinforced concrete exposed to high chloride environment. *Construction and Building Materials*, 303, 124461. <https://doi.org/10.1016/j.conbuildmat.2021.124461>
- [12] Teymouri, F., Allahkaram, S. R., Shekarchi, M., Azamian, I., & Johari, M. (2021). A comprehensive study on the inhibition behaviour of four carboxylate-based corrosion inhibitors focusing on efficiency drop after the optimum concentration for carbon steel in the simulated concrete pore solution. *Construction and Building Materials*, 296, 123702. <https://doi.org/10.1016/j.conbuildmat.2021.123702>
- [13] Harilal, M., et al. (2021). The chloride-induced corrosion of a fly ash concrete with nanoparticles and corrosion inhibitor. *Construction and Building Materials*, 274, 122097. <https://doi.org/10.1016/j.conbuildmat.2020.122097>
- [14] Wang, H., et al. (2020). Study on the influence of compound rust inhibitor on corrosion of steel bars in chloride concrete by electrical parameters. *Construction and Building Materials*, 262, 120763. <https://doi.org/10.1016/j.conbuildmat.2020.120763>
- [15] Song, Z., et al. (2021). Using ultrasonic wave to trigger microcapsule inhibitor against chloride-induced corrosion of carbon steel in simulated concrete pore solution. *Construction and Building Materials*, 311, 125331. <https://doi.org/10.1016/j.conbuildmat.2021.125331>
- [16] Hu, J., et al. (2021). The effect of organic core-shell corrosion inhibitors on corrosion performance of the reinforcement in simulated concrete pore solution. *Construction and Building Materials*, 267, 121011. <https://doi.org/10.1016/j.conbuildmat.2020.121011>
- [17] Ngo, T. T., Tran, N. T., Kim, D. J., & Pham, T. C. (2021). Effects of corrosion level and inhibitor on pullout behavior of deformed steel fiber embedded in high-performance concrete. *Construction and Building Materials*, 280, 122449. <https://doi.org/10.1016/j.conbuildmat.2021.122449>
- [18] Mohamed, A., Visco, D. P., & Bastidas, D. M. (2022). Effect of cations on the activity coefficient of no2-/no3- corrosion inhibitors in simulated concrete pore solution: An electrochemical thermodynamics study. *Corrosion Science*, 110476. <https://doi.org/10.1016/j.corsci.2022.110476>
- [19] Lapiro, I., Mezhev, A., & Kovler, K. (2022). Performance of corrosion inhibitors in reinforced concrete elements under electrical voltage. *Construction and Building Materials*, 342, 127656. <https://doi.org/10.1016/j.conbuildmat.2022.127656>



- [20] Das, J. K., & Pradhan, B. (2022). Study on influence of nitrite and phosphate-based inhibiting admixtures on chloride interaction, rebar corrosion, and microstructure of concrete subjected to different chloride exposures. *Journal of Building Engineering*, 50, 104192. <https://doi.org/10.1016/j.jobe.2022.104192>
- [21] Zhang, Y., et al. (2022). Inhibitor loaded functional HNTs modified coatings towards corrosion protection in reinforced concrete environment. *Progress in Organic Coatings*, 170, 106971. <https://doi.org/10.1016/j.porgcoat.2022.106971>
- [22] Wang, X. Y., Lee, S., & Cho, H. (2021). Penetration properties and injecting conditions of corrosion inhibitor for concrete. *Construction and Building Materials*, 284, 122761. <https://doi.org/10.1016/j.conbuildmat.2021.122761>
- [23] Yang, P., Gao, X., Wang, S., Su, J. F., & Wang, L. Q. (2022). Novel waterproof bituminous coating using self-healing microcapsules containing ultraviolet light curing agent. *Construction and Building Materials*, 329, 127189. <https://doi.org/10.1016/j.conbuildmat.2022.127189>
- [24] Zamanizadeh, H. R., Shishesaz, M. R., Danaee, I., & Zaarei, D. (2015). Investigation of the corrosion protection behavior of natural montmorillonite clay/bitumen nanocomposite coatings. *Progress in Organic Coatings*, 78, 256–260. <https://doi.org/10.1016/j.porgcoat.2014.08.011>
- [25] Kunthawatwong, R., et al. (2022). Recycled non-biodegradable polyethylene terephthalate waste as fine aggregate in fly ash geopolymers and cement mortars. *Construction and Building Materials*, 328, 127084. <https://doi.org/10.1016/j.conbuildmat.2022.127084>
- [26] Yu, S., Sanjayan, J., & Du, H. (2022). Effects of cement mortar characteristics on aggregate-bed 3D concrete printing. *Construction and Building Materials*, 332, 127405. <https://doi.org/10.1016/j.conbuildmat.2022.127405>
- [27] Subharaj, C., Logesh, M., Abdul Munaf, A., Srinivas, J., & Gnanaraj, S. J. P. (2022). Sustainable approach on cement mortar incorporating silica fume, LLDPE and sisal fiber. *Materials Today: Proceedings*. <https://doi.org/10.1016/j.matpr.2022.06.361>
- [28] Klyuev, S., et al. (2022). Fresh and mechanical properties of low-cement mortars for 3D printing. *Construction and Building Materials*, 338, 127644. <https://doi.org/10.1016/j.conbuildmat.2022.127644>
- [29] Nasir, M., et al. (2022). Engineered cellulose nanocrystals-based cement mortar from office paper waste: Flow, strength, microstructure, and thermal properties. *Journal of Building Engineering*, 51, 104345. <https://doi.org/10.1016/j.jobe.2022.104345>
- [30] Astuti, P., et al. (2024). Engineering properties of seawater-mixed mortar with batching plant residual waste as aggregate replacement. *SINERGI*, 28(2), 381. <https://doi.org/10.22441/sinergi.2024.2.017>
- [31] ASTM C4137. (2007). Standard test method for flow of hydraulic cement mortar. *ASTM International*.
- [32] SNI 1973:2016. (2016). Metode Uji Densitas, Volume Produksi Campuran dan Kadar Udara (Gravimetrik) Beton. *Badan Standardisasi Nasional*.
- [33] Elsener, B. (2001). Half-cell potential mapping to assess repair work on RC structures. *Construction and Building Materials*, 15(2–3), 133–139. [https://doi.org/10.1016/s0950-0618\(00\)00062-3](https://doi.org/10.1016/s0950-0618(00)00062-3)

Paper submitted: 25.04.2023.

Paper accepted: 12.06.2024.

This is an open access article distributed under the CC BY 4.0 terms and conditions